Am J Cancer Res 2026;16(3):905-919
www.ajcr.us /ISSN:2156-6976/ajcr0171121

Original Article

TNFAIP1 suppresses hepatocellular carcinoma progression via the PXR/CYP3A4 signaling axis

Qian Nie[1], Yiping Guo[1], Haowen Xiao[1], Dini Zhang[1], Haiyue Li[1], Ling Wang[2]

[1]The National & Local Joint Engineering Laboratory of Animal Peptide Drug Development, College of Life Science, Hunan Normal University, Changsha 410081, Hunan, China; [2]Hunan Provincial Key Laboratory of The Research and Development of Novel Pharmaceutical Preparations, Changsha Medical University, Changsha 410219, Hunan, China

Received December 30, 2025; Accepted March 17, 2026; Epub March 25, 2026; Published March 30, 2026

Abstract: Hepatocellular carcinoma (HCC) is characterized by poor prognosis and limited effective treatment options, necessitating a deeper understanding of its pathogenesis. This study focuses on tumor necrosis factor-α-induced protein 1 (TNFAIP1) and cytochrome P450 3A4 (CYP3A4) in HCC, aiming to investigate their association and functional roles in tumor progression. Bioinformatics analyses and experimental validation revealed that both TNFAIP1 and CYP3A4 are downregulated in HCC, and that TNFAIP1 positively regulates CYP3A4 expression. TNFAIP1 knockout not only decreased CYP3A4 expression but also significantly impaired the ability of rifampicin (RIF), an upstream nuclear receptor-pregnane X receptor (PXR) agonist, to induce CYP3A4, indicating that TNFAIP1 is an essential regulator of PXR/CYP3A4 pathway. Co-immunoprecipitation (Co-IP) experiment further confirmed the direct interaction between TNFAIP1 and PXR. TNFAIP1 knockout promoted HCC cell proliferation, migration, invasion, and epithelial-mesenchymal transition (EMT), while suppressing apoptosis; these effects were partially attenuated by pharmacological activation of PXR or genetic overexpression of CYP3A4. In vivo experiments demonstrated that overexpression of Tnfaip1 upregulated the Pxr/Cyp3a11 pathway and inhibited tumor growth, whereas Tnfaip1 knockout suppressed this pathway. This study identified TNFAIP1-PXR-CYP3A4 as a novel tumor-suppressive axis in HCC, providing potential molecular targets for HCC diagnosis and treatment.

Keywords: Hepatocellular carcinoma, tumor suppressor, cytochrome P450 3A4, tumor necrosis factor α-induced protein 1, pregnane X receptor

Introduction

Hepatocellular carcinoma (HCC) is the most common type of liver cancer, accounting for about 90% of all cases. Globally, liver cancer ranks as the fourth leading cause of cancer-related death [1, 2]. The pathogenesis of HCC is driven by a complex interplay of metabolic risk factors, environmental exposures, chronic viral infections, exogenous toxins, metabolic disorders, and immune-mediated liver injury [3-7]. Current treatment strategies for HCC include surgical resection, local regional therapies, targeted drugs, and immune checkpoint inhibitors [8-10]. However, most patients are diagnosed at intermediate or advanced stages, and existing therapeutic options are often limited by suboptimal efficacy, high recurrence rates, and the development of drug resistance, resulting in poor long-term survival outcomes [11, 12]. Therefore, it is of great significance to comprehensively elucidate the molecular mechanisms underlying HCC progression and identify novel prognostic biomarkers and treatment targets.

Tumor necrosis factor-α induced protein 1 (TNFAIP1), located at the chromosome 17q11.2 locus, encodes a protein composed of 316 amino acids [13]. It is involved in multiple biological pathways, including DNA synthesis and cell migration [14]. Increasing evidence indicates that TNFAIP1 plays a regulatory role in tumorigenesis and tumor development, making it a research focus. TNFAIP1 is highly expressed in normal cells, but its expression is markedly downregulated, by approximately 10-50 fold, in multiple cancer cell lines, such as HepG2 and SW480, and is consistently reduced in various

https://doi.org/10.62347/FSIQ3194

malignancies, including HCC and lung cancer [15]. Previous studies have demonstrated that TNFAIP1 suppresses HCC progression by inhibiting the NF-κB and p38/JNK MAPK signaling pathways [16, 17]. However, additional regulatory mechanisms of TNFAIP1 in HCC remain to be further elucidated.

Cytochrome P450 3A4 (CYP3A4) is the most important enzyme in drug metabolism, metabolizing approximately 50% of clinically used medicines [18-20]. Its expression is primarily regulated by the pregnane X receptor (PXR) [21], a nuclear receptor that upon activation, promotes transcription and expression of CYP3A4 [22]. Emerging evidence has identified CYP3A4 as a candidate biomarker associated with high risk and poor prognosis in HCC [23-25]. Functionally, overexpression of CYP3A4 suppresses tumor cell proliferation and epithelial-mesenchymal transition (EMT), whereas its downregulation promotes tumor progression [26, 27]. Nevertheless, the upstream regulatory network governing CYP3A4 expression in HCC remains incompletely understood.

Given that both TNFAIP1 and CYP3A4 possess tumor-suppressive potential, we hypothesize that TNFAIP1 may exert antitumor effects by regulating CYP3A4 via PXR-related pathways. This study aims to validate the expression patterns of TNFAIP1 and CYP3A4 in HCC, investigate the regulatory relationship between TNFAIP1 and CYP3A4 - particularly through PXR - and confirm their functional synergy in HCC progression using *in vitro* and *in vivo* experiments. Ultimately, this study seeks to establish the TNFAIP1-PXR-CYP3A4 axis as a novel inhibitory mechanism in HCC, thereby providing new theoretical insights into the diagnosis and targeted therapy of HCC.

Materials and methods

Online data analysis

Based on The Cancer Genome Atlas (TCGA) and Genotype-Tissue Expression (GTEx) databases, the differential expression of CYP3A4 in various tumor types and their corresponding normal tissues was evaluated using the GEPIA online analysis platform. Additionally, four HCC gene expression datasets (GSE14520, GSE45267, GSE64041, and GSE84598) were downloaded from the Gene Expression Omnibus (GEO) database. Differentially expressed genes (DEGs) were analyzed using R software, and the expression levels of CYP3A4 in HCC and matched adjacent non-tumorous tissues were visualized.

Cell culture

Cells were maintained in DMEM (Gibco) supplemented with 10% fetal bovine serum and 1% penicillin-streptomycin. Cells were incubated at 37°C in a humidified atmosphere containing 5% CO_2. The human immortalized normal hepatocyte cell line THLE-2 and two HCC cell lines, HepG2 and SMMC-7721, were obtained from the Shanghai Cell Bank.

TNFAIP1 was silenced in SMMC-7721 cells via the CRISPR/Cas9 approach, and stable cell lines (SMMC7721-Control and SMMC7721-KO-TNFAIP1) were established and cultured under the same cultivation environments.

Quantitative real-time PCR (qRT-PCR)

Total RNA was extracted from cell and liver tissue samples using Trizol reagent (Takara) according to the manufacturer's protocol. RNA quality and concentration were detected using a NanoDrop spectrophotometer (Thermo). Complementary DNA (Cdna) was synthesized from 1 μg of total RNA using the reverse transcription kit (Novoprotein), and then incubated at 37°C for 50 min, followed by denaturation at 95°C for 6 min.

RT-qPCR was performed using a Bio-Rad real-time PCR system with NovoStart®SYBR Green qPCR Master Mix Plus reagent. Each 10 μL reaction mixture contained 5 μl of 2 × SYBR mix, 0.4 μl of each primer (10 μM), 4 μl of dilute cDNA, and 0.2 μl of RNase-free water. Cycling conditions: 95°C for 1 min, 40 cycles of 95°C for 20 s, 55-60°C for 20 s, and 72°C for 30 s, followed by melting curve analysis. GAPDH served as the internal reference gene, and relative expressions of genes were quantified using the 2^(-ΔΔCt) method. The specific primer sequences are listed in Table S1.

Western blot analysis

Cells or tissue samples were lysed in RIPA buffer containing protease inhibitors. Protein concentration were determined using a Bradford protein detection kit (BCA method). Equal

amounts of protein (30 μg) was separated by SDS-PAGE and transferred to PVDF membranes, which were then blocked in 5% skim milk at room temperature for 1 h, followed by incubation with primary antibodies overnight at 4°C. After washing, membranes were incubated with HRP-conjugated secondary antibodies for 1 h at room temperature. After washing, protein bands were visualized using ECL reagent on a Tanon-5500 imaging instrument, and band intensities were assessed using Image Lab software (Bio-Rad), normalized to GAPDH/β-actin. All antibodies were utilized at their supplier-specified dilutions.

Co-immunoprecipitation (Co-IP)

To assess interactions among TNFAIP1, PXR, and other molecules, Co-IP assay were performed. Cells were washed twice with ice-cold PBS and lysed in IP lysis buffer. After centrifugation, the supernatants were collected. For immunoprecipitation, the lysates were incubated with specific antibodies against TNFAIP1 (Proteintech, 2 μg per reaction) or PXR (Santa Cruz Biotechnology, 2 μg per reaction) overnight at 4°C with rotation. Normal IgG served as the isotype control under the same conditions. Next, Protein A/G agarose beads were added to the lysis buffer and incubated on ice for another two hours. Bead-bound complexes were extensively washed with lysis buffer, and obtained proteins were eluted by heating in 1 × SDS loading buffer. Both the input and eluate samples were subjected to western blot assay using antibodies against TNFAIP1 (1:1000), PXR (1:500), and GAPDH (1:5000) to identify interaction partners. Lysates from TNFAIP1-knockout SMMC-7721 cells were used for further specificity testing.

MTT assay

Cells were treated with rifampicin (RIF; McLean Reagent Company) at different concentrations (5, 10, 20, 50, 100, 150 μM) for 24 or 48 hours. Subsequently, 0.5 mg/mL MTT reagent was added and further incubated for an additional 4 hours. MicroPlate Reader was used for measuring OD at 492 nm.

CYP3A4 overexpression

To verify whether TNFAIP1 regulates CYP3A4 function, a CYP3A4 overexpression plasmid was constructed. Full-length human CYP3A4 cDNA was cloned into the PCMV3-C-Flag plasmid (Sino Biological). Wild-type or TNFAIP1-knockdown SMMC-7721 cells were co-transfected with PCMV3-C-Flag-CYP3A4 or empty vector using Lipofectamine 3000 reagents. Stable cell lines were then obtained after G418 screening. Expression of Flag-tagged CYP3A4 was confirmed by western blot employing an anti-Flag antibody. These stable cells were then used for functional rescue assays.

Transwell invasion assay

The upper chambers were pre-coated with Matrigel, and 5 × 10^4 cell were seeded into each well. The lower chamber contained medium supplemented with 10% fetal bovine serum as a chemoattractant. After 24 hours, cells remaining on the upper surface were removed, and invaded cells were fixed and stained with crystalline violet; Five random fields per well were imaged and counted under a microscope.

Wound healing test

When cells reached 100% confluency, a straight scratch was made with a disposable sterile 200 μL micro-pipette tip. Cells were rinsed with PBS and incubated in serum-free medium. Images were captured at 0, 24 and 48 hours to calculate the percentage of wound closure.

Colony formation test

Cells were inoculated at a density of 2000 cells/well in a 6-well plate and cultured for two weeks, with culture medium replaced regularly. Once visible colonies appeared, they were fixed with 4% paraformaldehyde and stained using 0.4% crystal violet (Shanghai Biotech Co., Ltd.). Then, colonies with more than 500 cells were counted.

Hoechst staining

Cells were fixed for 15 min and then stained with Hoechst 33258 for another 15 minutes. Subsequently, after the PBS washes, apoptotic cells were quantified.

Animal experiments

Specific pathogens-free (SPF) C57BL/6J mice were purchased from Beijing SPF Biotechnology Co., Ltd. Mice were housed under specific pathogen-free conditions at (22 ± 2°C), relative

humidity of (50 ± 10%), 12 h light/12 h dark cycle, with ad libitum access to food and water. Tnfaip1-KO mice, generated BY Cyagen Biosciences, were bred in our laboratory. All animal experiments were approved by the Animal Ethics Committee of Hunan Normal University.

DEN/CCl4-induced HCC model

Fourteen-day-old C57BL/6J mice were randomly divided into three groups: control, diethylnitrosamine (DEN), and DEN plus adeno-associated virus carrying the Tnfaip1 gene (DEN + AAV-Tnfaip1). Mice in the DEN group received intraperitoneal injections of DEN (50 mg/kg, dissolved in saline), while control mice received saline only. Two weeks later, mice in the DEN and DEN + AAV-Tnfaip1 groups were administered intraperitoneal injections of 10% CCl_4 twice weekly until day 98, whereas control mice received equivalent volumes of corn oil. Histological assessment confirmed that by day 98, livers had developed dysplastic nodules and early hepatocellular carcinoma foci, representing a progression from pre-neoplastic lesions to established tumors [28-30].

On day 98, mice in the DEN + AAV-Tnfaip1 group were injected with AAV-Tnfaip1 via the tail vein, while control and DEN groups received empty vector. This intervention timing was selected to model a clinically relevant scenario of therapeutic intervention in early-stage HCC, allowing evaluation of Tnfaip1's potential to regress established early lesions [28-30]. On day 133 of the experiment, mice were euthanized by cervical dislocation, and liver tissue and serum were collected. Serum alanine aspartate aminotransferase (AST) and aminotransferase (ALT) levels were measured according to the manufacturer's instructions (Nanjing, Jiancheng).

Hematoxylin and Eosin (H&E) staining

Liver tissues were fixed, paraffin-embedded, sectioned, and stained with hematoxylin and eosin solution. Histopathological evaluation was performed under a light microscope.

Extraction of total RNA and protein from mouse liver

Approximately 30 mg of liver tissue was homogenized in Trizol reagent (Takara) using a tissue homogenizer (Ningbo Xinzhi) to extract total RNA following the manufacturer's instructions. For protein extraction, approximately 50 mg of tissue was lysed in RIPA lysis buffer containing protease inhibitors. RNA and protein concentrations were quantified using a NanoDrop spectrophotometer (Thermo) and the BCA assay, respectively.

Statistical analysis

All data were presented as mean ± standard deviation (SD). Comparisons between two groups were performed using Student's t-test, while comparisons among multiple groups were performed using one-way analysis of variance (ANOVA) followed by Dunnett's post hoc test. For experiments involving repeated measurements over multiple time points, repeated measures ANOVA was used to assess differences between groups across time. All experiments were repeated at least three times. Statistical analyses and graphical presentations were performed using GraphPad Prism 8. A p-value < 0.05 was considered statistically significant.

Results

TNFAIP1 positively regulates CYP3A4 expression in HCC cells

We first investigated the potential association between TNFAIP1 and CYP3A4 in HCC using bioinformatics analysis and clinical evidence. Analysis of TCGA and GTEx databases revealed that CYP3A4 expression was markedly lower in HCC (LIHC) tissues compared to normal liver tissues (**Figure 1A**). This downregulation was further confirmed across four independent HCC gene expression datasets from the GEO database (**Figure 1B**). In our previous study analyzing 80 paired HCC patient tissues, TNFAIP1 expression was found to be significantly downregulated in tumor tissues [17]. To extend these observations to cellular models, we examined the expression of both TNFAIP1 and CYP3A4 in the human immortalized normal hepatocyte cell line THLE-2 and in HCC cell lines (HepG2 and SMMC-7721). The expression levels of both TNFAIP1 and CYP3A4 were relatively lower in the HCC cells compared to THLE-2 cells (**Figures 1C-E**, **2A-C**). Furthermore, analysis of TCGA-LIHC tumor samples showed a weak but statistically significant positive cor-

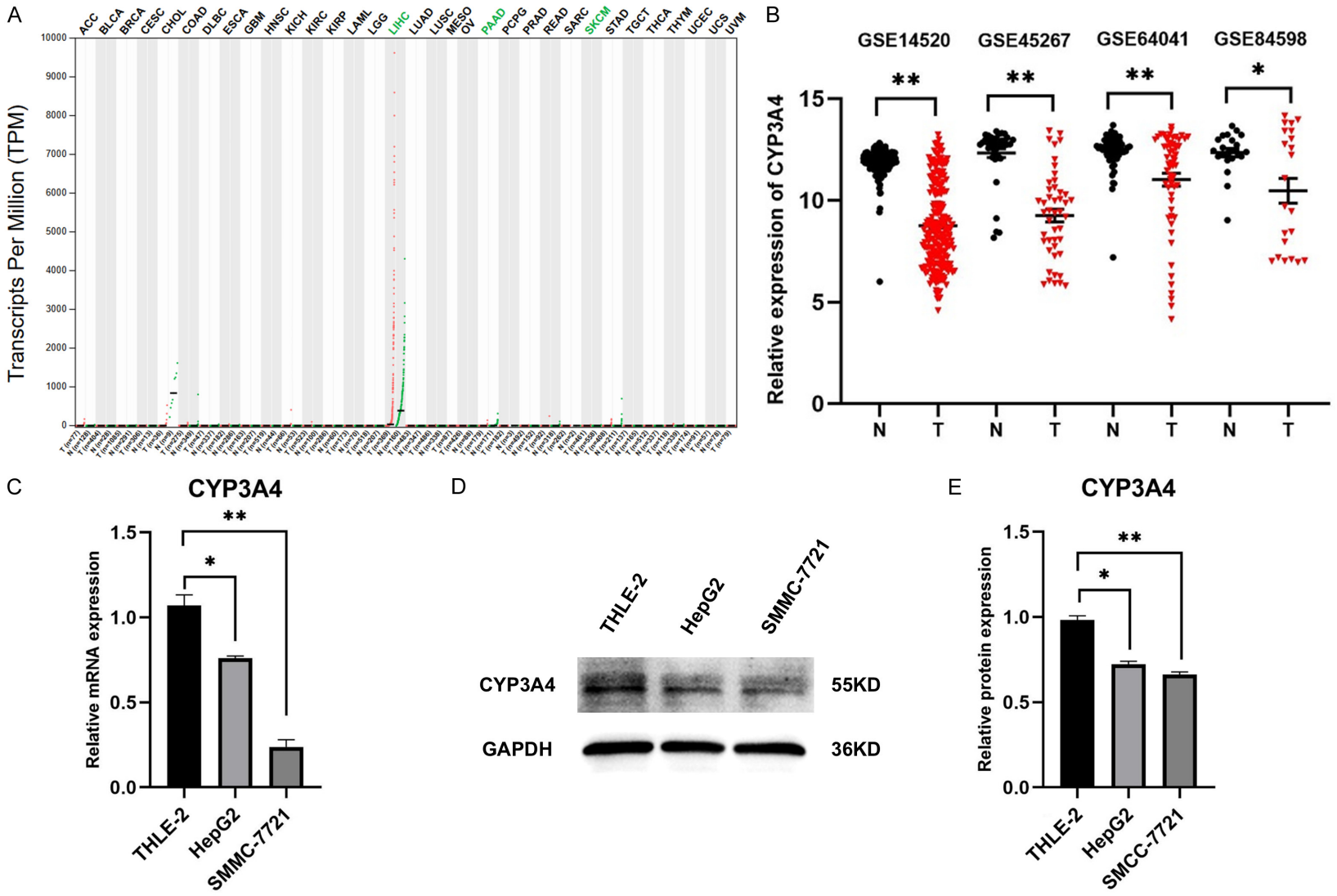

Figure 1. Cytochrome P450 3A4 (CYP3A4) expression is downregulated in hepatocellular carcinoma (HCC) tissues and cell lines. A. Differential expression of the CYP3A4 gene in tumor versus non-tumor tissues from patients with various cancers; B. CYP3A4 expression in tumor and adjacent normal tissues from HCC patients; C. CYP3A4 mRNA levels in THLE-2, HepG2, and SMMC-7721 cells; D, E. CYP3A4 protein levels in THLE-2, HepG2, and SMM-C7721 cells. $^{*}P < 0.05$, $^{**}P < 0.01$.

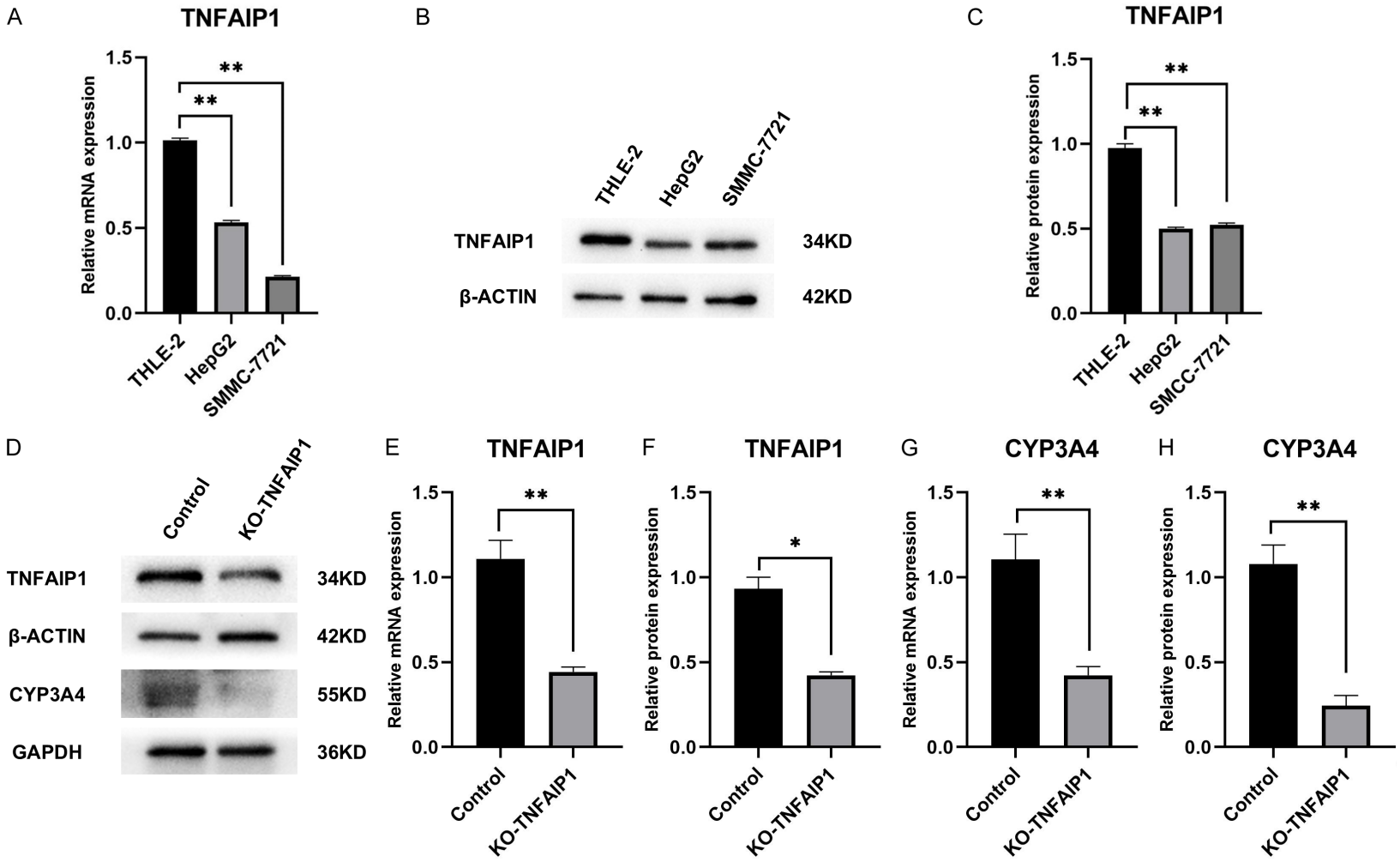

Figure 2. Expression of tumor necrosis factor-α-induced protein 1 (TNFAIP1) and CYP3A4 in hepatocyte cell lines. A. TNFAIP1 mRNA levels in THLE-2 HepG2, and SMMC-7721 cells; B, C. TNFAIP1 protein levels in THLE-2, HepG2, and SMMC-7721 cells; D. TNFAIP1 and CYP3A4 protein levels in SMMC7721-Control and KO-TNFAIP1 cell lines; E. TNFAIP1 mRNA levels in SMMC7721-Control/KO-TNFAIP1 cell lines; F. Quantitative analysis of TNFAIP1 protein expression levels in SMMC7721-Control/KO-TNFAIP1 cell lines; G. CYP3A4 mRNA levels in SMMC7721-Control/KO-TNFAIP1 cell lines; H. Quantitative analysis of CYP3A4 protein expression levels in SMMC7721-Control/KO-TNFAIP1 cell lines. $^{*}P < 0.05$, $^{**}P < 0.01$.

relation between TNFAIP1 and CYP3A4 mRNA expression (Spearman R = 0.23, p = 1.1e-05; Figure S1). Together, these data from public databases, clinical samples, and cell lines suggest a potential regulatory relationship between TNFAIP1 and CYP3A4.

To directly test whether TNFAIP1 regulates CYP3A4, we generated a stable TNFAIP1-knockout (KO) cell line in SMMC-7721 cells using CRISPR/Cas9 technology. Compared to control cells, the loss of TNFAIP1 led to a significant reduction in CYP3A4 expression at both the mRNA and protein levels (**Figure 2D-H**). These results indicate that TNFAIP1 acts as a positive regulator of CYP3A4 expression in HCC cells.

TNFAIP1 is required for the functional responsiveness of the PXR/CYP3A4 axis

CYP3A4 is a well-established transcriptional target of the nuclear receptor PXR. To investigate the role of TNFAIP1 in regulating the PXR/CYP3A4 axis, SMMC-7721 cells were treated with RIF, a specific agonist of PXR. An MTT assay was first performed to determine non-cytotoxic RIF concentration (**Figure 3A**). In control SMMC-7721 cells, RIF treatment significantly increased the expression of both PXR and its downstream target gene CYP3A4 in a dose-dependent manner, with the most pronounced induction observed at 20 μM RIF (**Figure 3B-F**). We then evaluated the effects of RIF under conditions of TNFAIP1 deficiency. Compared to control cells, TNFAIP1 knockout not only reduced the basal expression levels of both PXR and CYP3A4 but also significantly attenuated the RIF-induced upregulation of CYP3A4. Notably, TNFAIP1 knockout also impaired the RIF-mediated increase in PXR expression itself (**Figure 3G-K**). These findings suggest that TNFAIP1 is critical for maintaining the functional output of the PXR/CYP3A4 signaling axis, as its loss compromises both the basal expression and agonist-responsive induction of this pathway.

To explore whether TNFAIP1 interacts directly with PXR, we performed Co-IP assays. In SMMC-7721 cells, antibodies targeting TNFAIP1 or PXR effectively co-precipitated the reciprocal protein, whereas non-specific IgG did not (**Figure 3L**). Importantly, this interaction was not detected in TNFAIP1-knockout cells, confirming its specificity. This discovery provides direct evidence for a molecular interaction between TNFAIP1 and PXR.

Both pharmacological activation and genetic restoration of CYP3A4 attenuated pro-tumorigenic phenotypes induced by TNFAIP1 knockout

To investigate whether CYP3A4 acts as a downstream effector mediating the anti-tumor function of TNFAIP1, both pharmacological and genetic approaches were conducted. First, intervention with the PXR agonist RIF in TNFAIP1-knockout cells showed that RIF treatment was associated with a significant attenuation of multiple pro-tumorigenic phenotypes. Specifically, RIF effectively inhibited cell migration, invasion, and clonogenic ability that enhanced by TNFAIP1 knockout (**Figure 4A-D**). It also partially reversed changes in EMT-related proteins expression (**Figure 4E**) and promoted the recovery of cell apoptosis (**Figure 5A**, **5B**). To further clarify whether this phenotypic rescue specifically mediated by CYP3A4 rather than other effects following PXR activation by RIF, we overexpressed CYP3A4 in TNFAIP1-knockdown cells (**Figure 5C**). Genetic restoration of CYP3A4 alone was sufficient to partially reverse the enhanced clonogenicity (**Figure 5D**, **5E**) and migration capacity (**Figure 5F**, **5G**) induced by TNFAIP1 deficiency. In summary, both pharmacological activation of the PXR/CYP3A4 axis and genetic restoration of CYP3A4 alleviated the impact of TNFAIP1 loss on specific phenotypes. These results support the conclusion that CYP3A4 is an important downstream effector of TNFAIP1-mediated tumor suppression.

In vivo evidence demonstrates that Tnfaip1 suppresses HCC progression via the Pxr/Cyp3a11 axis

To examine the *in vivo* regulatory relationship between TNFAIP1 and CYP3A4, and their functional roles in HCC, a DEN-CCl_4-induced HCC model was established in mice, followed by intervention with tail vein injection of AAV-Tnfaip1 (**Figure 6A**). In tumor-bearing livers, Tnfaip1 expression was downregulated, accompanied by reduced expression of Pxr and Cyp3a11 (**Figure 6B-D**), suggesting suppression of this signaling pathway during HCC progression. To determine whether Tnfaip1 acts as

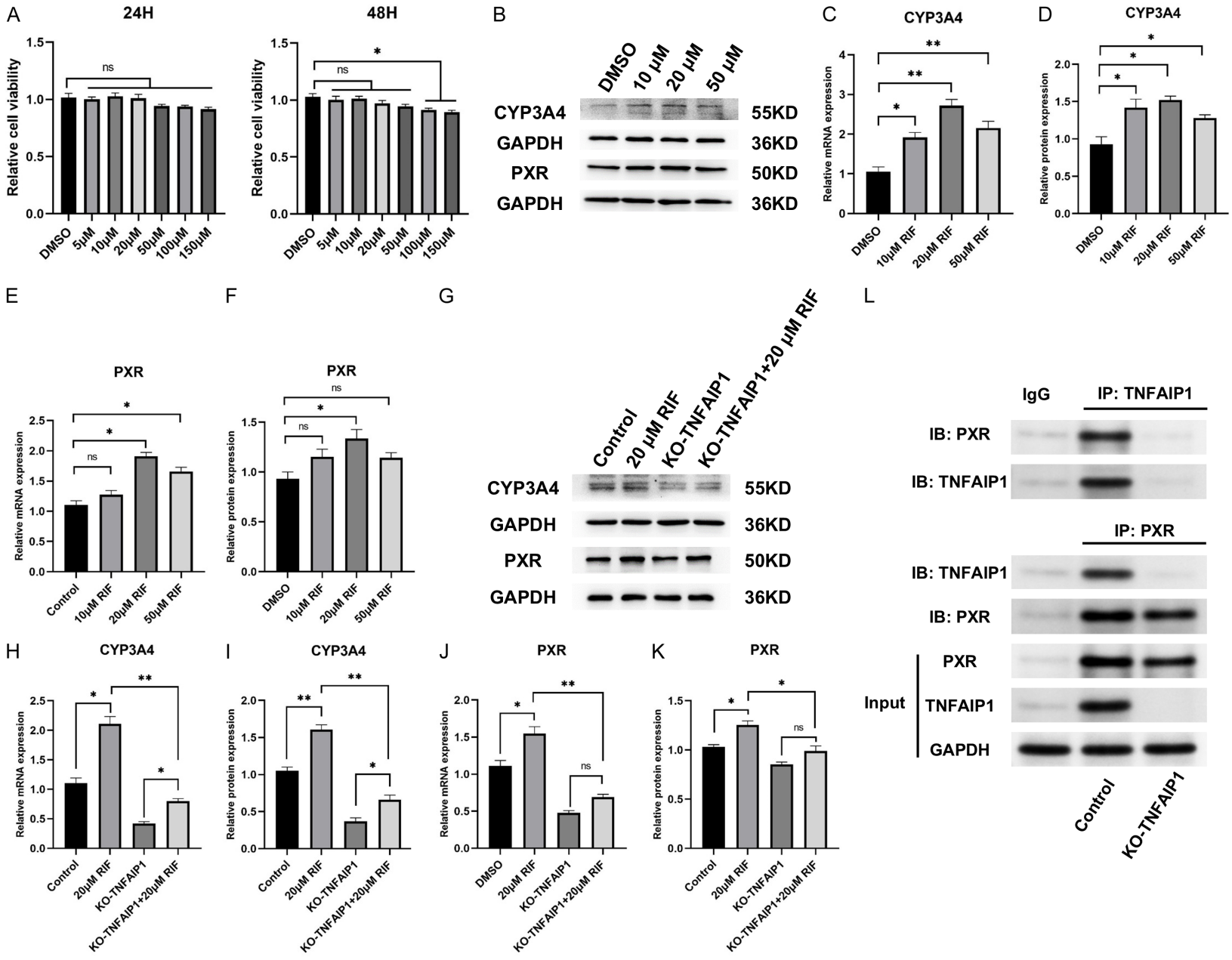
A
24H
48H
Relative cell viability
DMSO
5μM
10μM
20μM
50μM
100μM
150μM
B
DMSO
10 μM
20 μM
50 μM
CYP3A4
GAPDH
PXR
55KD
36KD
50KD
C
CYP3A4
Relative mRNA expression
10μM RIF
20μM RIF
50μM RIF
D
CYP3A4
Relative protein expression
E
PXR
Control
F
PXR
G
Control
20 μM RIF
KO-TNFAIP1
KO-TNFAIP1+20 μM RIF
H
CYP3A4
20μM RIF
KO-TNFAIP1
KO-TNFAIP1+20μM RIF
I
CYP3A4
J
PXR
K
PXR
L
IgG
IP: TNFAIP1
IB: PXR
IB: TNFAIP1
IP: PXR
Input
Control
KO-TNFAIP1

Figure 3. TNFAIP1 knockout attenuated rifampicin (RIF)-augmented CYP3A4 expression. A. Cell proliferation of SMMC-7721 cells treated with different concentrations of RIF at 24 h and 48 h; B. Protein levels of CYP3A4 and pregnane X receptor (PXR) in SMMC-7721 cells treated with different concentrations of RIF; C. CYP3A4 mRNA levels in SMMC-7721 cells treated with different concentrations of RIF; D. Quantitative analysis of CYP3A4 protein expression levels after RIF treatment; E. mRNA levels of PXR in SMMC-7721 cells treated with different concentrations of RIF; F. Quantitative analysis of PXR protein expression levels after treatment with different concentrations of RIF; G. Protein levels of CYP3A4 and PXR in SMMC7721-Control/KO-TNFAIP1 cell lines treated with 20 μM RIF; H. mRNA levels of CYP3A4 in SMMC7721-Control/KO-TNFAIP1 cell lines treated with 20 μM RIF; I. Quantitative analysis of CYP3A4 protein expression levels after 20 μM RIF treatment; J. mRNA levels of PXR in SMMC7721-Control/KO-TNFAIP1 cell lines after 20 μM RIF treatment; K. Quantitative analysis of PXR protein expression levels after 20 μM RIF treatment. L. Co-IP assay demonstrating the interaction between endogenous TNFAIP1 and PXR in SMMC-7721 cells. $^{*}P < 0.05$, $^{**}P < 0.01$.

an upstream regulator of this pathway, AAV-mediated overexpression of Tnfaip1 was performed via tail vein injection in the HCC model mice. Following intervention, Tnfaip1 expression in the liver was successfully restored, accompanied by significant upregulation of Pxr and Cyp3a11 expression (**Figure 6B-D**). Phenotypically, Tnfaip1 overexpression significantly reduced hepatic tumor nodule formation (Figure S2A), decreased serum ALT and AST levels (Figure S2B), and ameliorated histopathological liver damage (Figure S2C). In addition, mRNA levels of liver cancer-associated biomarkers (AFP, Ccnd1, Fgf21, IL-6) were downregulated (Figure S2D). These findings suggest that restoration of Tnfaip1 exerts antitumor effects *in vivo* through activation of the Pxr/Cyp3a11 axis.

To further validate the regulatory role of Tnfaip1 *in vivo*, systemic knockout ($Tnfaip1^{-/-}$) mice were examined. Compared with wild-type (WT) mice, Tnfaip1 knockout resulted in significantly reduced expression levels of Pxr and Cyp3a11 in mouse liver (**Figure 6E-G**). Additionally, knockout of Tnfaip1 altered the expression of local liver immune components (complement factors C3, C5) and IL-6 (Figure S3), suggesting its potential involvement in broader immune microenvironment regulation. These findings indicate that Tnfaip1 is a critical upstream regulator of the Pxr/Cyp3a11 axis, and highlight the TNFAIP1-PXR-CYP3A4 signaling pathway as a novel mechanism for suppressing HCC.

Discussion

HCC accounts for 90% of primary liver cancers, and its clinical treatment remains a significant challenge. Current therapies yield suboptimal outcomes due to limited response rates and drug resistance [11, 12]. Therefore, elucidating novel therapeutic targets and mechanisms is crucial [1]. Integrating bioinformatics data with experimental validation, this study identified a TNFAIP1/PXR/CYP3A4 signaling axis that exerts a critical tumor-suppressive role in HCC.

Our findings reveal that CYP3A4 expression is downregulated in HCC tissues and cell lines, consistent with previous studies [23-25, 31-33], supporting its potential as a diagnostic and prognostic biomarker for HCC. CYP3A4 is responsible for approximately 50% of clinical drug metabolism [18-20]. Its overexpression can inhibit tumor cell proliferation and EMT, while its downregulation promotes tumor progression [26, 27]. However, the mechanism of its upstream regulatory network in HCC remains incompletely elucidated. Concurrently, this study confirms that the tumor suppressor TNFAIP1 is downregulated in HCC, which aligns with previous study reporting downregulated TNFAIP1 in multiple human cancers and its participation in tumor progression [14, 34]. Previous studies demonstrated that TNFAIP1 inhibited HCC progression by suppressing the NF-κB and p38/JNK MAPK pathways [16, 17]. However, this study reveals a novel mechanism by which TNFAIP1 exerts tumor-suppressive effects: acting as a key positive regulator, TNFAIP1 maintains normal CYP3A4 expression levels. Knockdown of TNFAIP1 leads to decreased CYP3A4 expression, linking these two independent tumor suppressors. Moreover, we elucidate the central mediating role of PXR in this regulatory relationship [22]. TNFAIP1 deficiency not only reduces PXR expression but also impairs the ability of the PXR agonist RIF to induce CYP3A4 transcription [35]. Critically, Co-IP assays provided direct evidence for the interaction between TNFAIP1 and PXR, offering a molecular basis for their functional coupling. These findings suggest that TNFAIP1 plays an

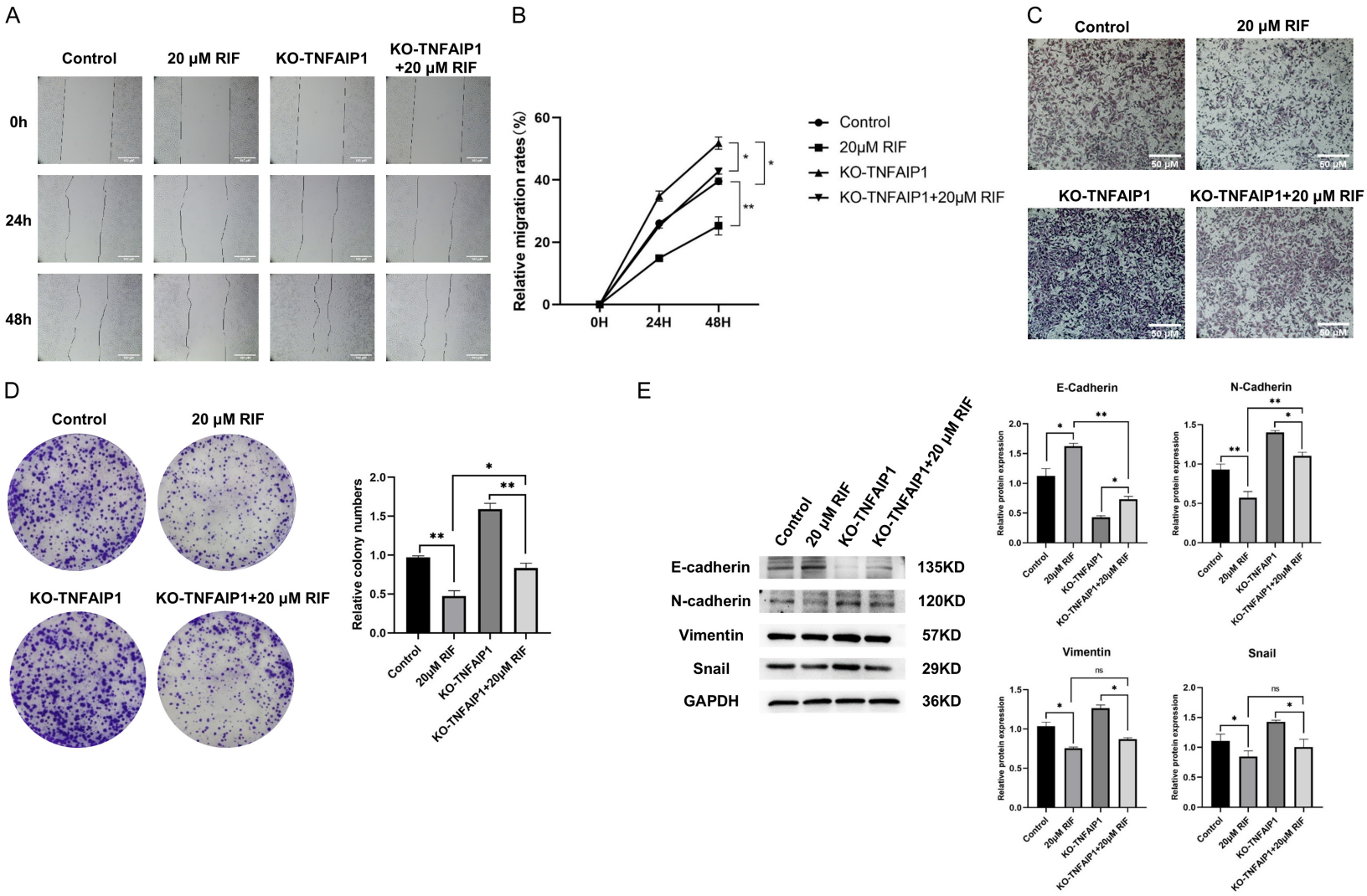

Figure 4. Pharmacological activation of the PXR/CYP3A4 axis attenuated TNFAIP1 knockout-induced migration, invasion, EMT, and proliferation. A. Migration in SMMC7721-Control/KO-TNFAIP1 cells treated with 20 μM RIF (scale bar = 100 μm; Magnification: ×100); B. Quantitative analysis of cell migration; C. Cell invasion in SMMC7721-Control/KO-TNFAIP1 cell lines treated with 20 μM RIF (scale bar = 50 μm; Magnification: ×400); D. Clonogenic assay of SMMC7721-Control/KO-TNFAIP1 cell lines treated with 20 μM RIF; E. Western blot analysis of EMT marker protein levels (E-cadherin, N-cadherin, vimentin, Snail) in SMMC7721-Control/KO-TNFAIP1 cell lines treated with 20 μM RIF. $^{*}P < 0.05$, $^{**}P < 0.01$.

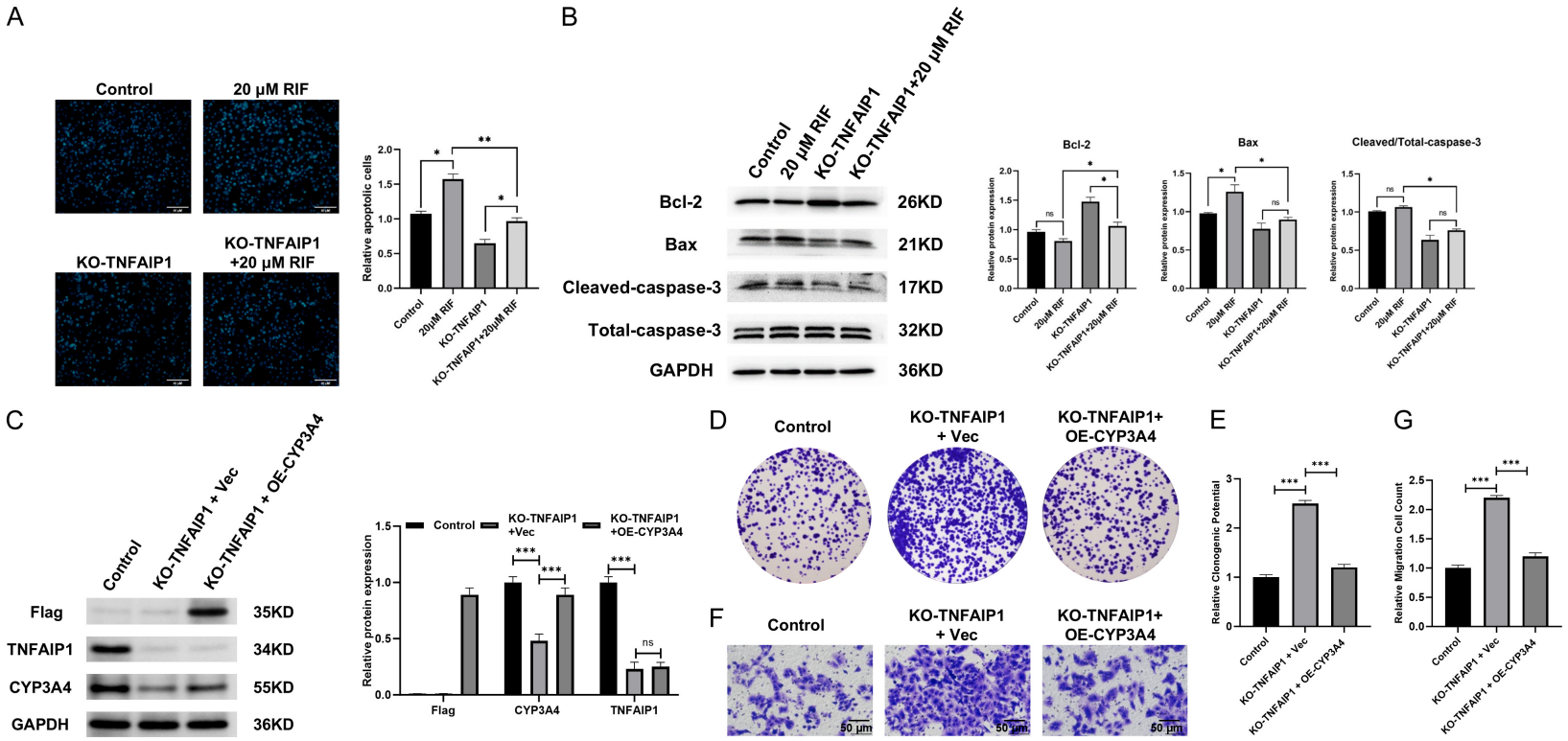

Figure 5. Genetic restoration of CYP3A4 mitigated pro-tumorigenic phenotypes in TNFAIP1 knockout cells. A. Apoptosis in SMMC7721-Control/KO-TNFAIP1 cell lines treated with 20 μM RIF (scale bar = 50 μm; Magnification: ×400); B. Protein levels of apoptosis-related proteins (Bcl-2, Bax, Cleaved/Total-caspase-3) in SMMC7721-Control/KO-TNFAIP1 cell lines treated with 20 μM RIF; C. Western blot validation of Flag-tagged CYP3A4 overexpression in SMMC7721-Control/KO-TNFAIP1 cell lines; D, E. Clonogenic assay of SMMC7721 control/KO-TNFAIP1 cell line overexpressing CYP3A4; F, G. Cell invasion in SMMC7721 control/KO-TNFAIP1 cell line overexpressing CYP3A4 (scale bar = 100 μM; Magnification: ×200). $^{*}P < 0.05$, $^{**}P < 0.01$, $^{***}P < 0.001$.

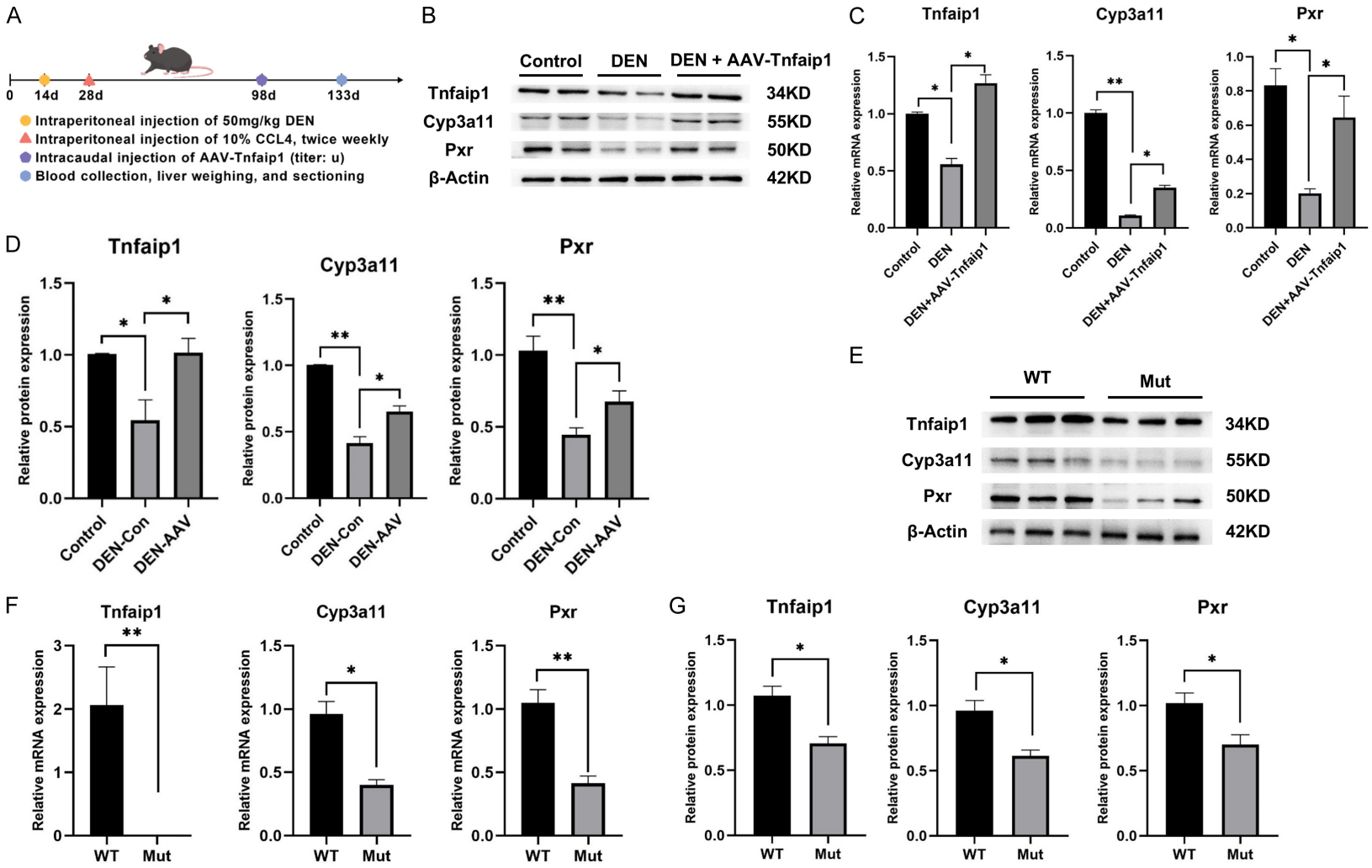

Figure 6. In vivo validation of Tnfaip1 as a positive regulator of the Pxr/Cyp3a11 axis and suppressor of HCC progression. A. Schematic of the DEN/CCl_4-induced HCC mouse model and AAV-Tnfaip1 intervention protocol; B. Protein levels of Tnfaip1, Cyp3a11, and Pxr in mouse liver tissue; C. mRNA levels of Tnfaip1, Cyp3a11, and Pxr in mouse liver tissue; D. Quantitative analysis of protein expression levels; E. Protein levels of Tnfaip1, Cyp3a11, and Pxr in liver tissues of WT and Mut mice; F. mRNA levels of Tnfaip1, Cyp3a11, and Pxr in liver tissues of WT and Mut mice; G. Quantitative analysis of protein expression levels. $^{*}P < 0.05$, $^{**}P < 0.01$.

important role in supporting the activity of the PXR/CYP3A4 axis.

The functional significance of the PXR/CYP3A4 axis downstream of TNFAIP1 was highlighted in our rescue experiments. Pharmacological activation of this axis with RIF significantly attenuated the pro-tumorigenic phenotypes induced by TNFAIP1 knockout, including enhanced EMT, proliferation, migration, and invasion, along with reduced apoptosis. To directly attribute these effects to CYP3A4, we genetically overexpressed CYP3A4 in TNFAIP1-deficient cells. This intervention alone was sufficient to partially reverse the enhanced clonogenicity and migration, providing more direct evidence for the involvement of CYP3A4 in mediating these cellular phenotypes. This indicates that impairment of the PXR/CYP3A4 axis is a major contributor to the oncogenic phenotype resulting from TNFAIP1 deficiency, with CYP3A4 downregulation being a pivotal component. Emerging evidence suggests that cytochrome P450 enzymes, including CYP3A4, can influence cell fate by metabolizing specific endogenous signaling molecules or by interacting with key cellular pathways [36, 37]. For instance, CYP3A4 may exert effects by metabolizing certain lipid precursors promoting EMT or proliferation, or by influencing the stability of transcription factors such as Snail. *In vivo* experiments further corroborated the significance of this regulatory axis. In a DEN/CCl_4-induced HCC mouse model, Tnfaip1 overexpression significantly upregulated Pxr/Cyp3a11 and inhibited tumor progression; conversely, systemic Tnfaip1 knockout impaired the expression of this axis. Collectively, these data support the functional relevance of the TNFAIP1-PXR-CYP3A4 signaling axis in HCC pathogenesis.

This study has certain limitations. First, while we employed genetic overexpression of CYP3A4 to strengthen the evidence for its specific role, the use of RIF (a broad-spectrum PXR agonist) may activate additional detoxification genes that contribute to the observed phenotypic effects. Therefore, further validation using CYP3A4-specific knockdown in TNFAIP1-deficient models would provide complementary evidence to clarify the necessity of CYP3A4 within this regulatory axis. Second, it remains to be determined whether the TNFAIP1-PXR-CYP3A4 axis interacts with other metabolic pathways, such as glycolysis [37, 38], or whether TNFAIP1 regulates a broader network of cytochrome P450 enzymes [39]. Third, while our study established a physical interaction between TNFAIP1 and PXR, future studies employing PXR promoter reporter assays and Co-IP are needed to elucidate the precise molecular mechanism by which TNFAIP1 regulates PXR transcriptional activity. Addressing these questions will offer a more comprehensive understanding of the tumor-suppressive mechanisms governed by TNFAIP1.

Conclusion

TNFAIP1 suppresses malignant progression in HCC by positively regulating the PXR/CYP3A4 signaling pathway. Disruption of this axis promotes tumorigenesis, while restoring its activity attenuates the cancerous phenotype. These findings establish the theoretical foundation for developing. Targeting TNFAIP1-PXR-CYP3A4 axis may provide novel insights into the development of targeted therapeutic strategies for HCC.

Acknowledgements

This study was supported by the Project of Changsha Science and Technology Bureau.

Disclosure of conflict of interest

None.

Address correspondence to: Ling Wang, Hunan Provincial Key Laboratory of The Research and Development of Novel Pharmaceutical Preparations, Changsha Medical University, No. 1501 Lei Feng Avenue, Xiangjiang New District, Changsha 410219, Hunan, China. E-mail: wangling081105@163.com

References

[1] Li Y, Wu Y, Zuo S, Zhao W, Liu J, Wang Y, Zhang X, Xu J, Sun F, Zhang D, Zhu S and Shen A. GRWD1 inhibits nucleolar stress and reduces the sensitivity of hepatocellular carcinoma to oxaliplatin. Genes Dis 2026; 13: 101725.

[2] Liu G, Long J, Liu C and Chen J. Development and verification of a nomogram for predicting portal vein tumor thrombosis in hepatocellular

carcinoma. Am J Transl Res 2024; 16: 7511-7520.
[3] Gao J, Zhang M, Chen Q, Ye K, Wu J, Wang T, Zhang P and Feng G. Integrating machine learning and molecular docking to decipher the molecular network of aflatoxin B1-induced hepatocellular carcinoma. Int J Surg 2025; 111: 4539-4549.
[4] Hussain SP, Schwank J, Staib F, Wang XW and Harris CC. TP53 mutations and hepatocellular carcinoma: insights into the etiology and pathogenesis of liver cancer. Oncogene 2007; 26: 2166-2176.
[5] Koshy A. Evolving global etiology of hepatocellular carcinoma (HCC): insights and trends for 2024. J Clin Exp Hepatol 2025; 15: 102406.
[6] Kulik L and El-Serag HB. Epidemiology and management of hepatocellular carcinoma. Gastroenterology 2019; 156: 477-491, e471.
[7] Lleo A, Leung PSC, Hirschfield GM and Gershwin EM. The pathogenesis of primary biliary cholangitis: a comprehensive review. Semin Liver Dis 2020; 40: 34-48.
[8] Chan LL, Kwong TT, Yau JCW and Chan SL. Treatment for hepatocellular carcinoma after immunotherapy. Ann Hepatol 2025; 30: 101781.
[9] Li B, Yan C, Zhu J, Chen X, Fu Q, Zhang H, Tong Z, Liu L, Zheng Y, Zhao P, Jiang W and Fang W. Anti-PD-1/PD-L1 blockade immunotherapy employed in treating hepatitis B virus infection-related advanced hepatocellular carcinoma: a literature review. Front Immunol 2020; 11: 1037.
[10] Llovet JM, De Baere T, Kulik L, Haber PK, Greten TF, Meyer T and Lencioni R. Locoregional therapies in the era of molecular and immune treatments for hepatocellular carcinoma. Nat Rev Gastroenterol Hepatol 2021; 18: 293-313.
[11] Bruix J, Gores GJ and Mazzaferro V. Hepatocellular carcinoma: clinical frontiers and perspectives. Gut 2014; 63: 844-855.
[12] Elsegood CL, Tirnitz-Parker JE, Olynyk JK and Yeoh GC. Immune checkpoint inhibition: prospects for prevention and therapy of hepatocellular carcinoma. Clin Transl Immunology 2017; 6: e161.
[13] Fagerberg L, Hallström BM, Oksvold P, Kampf C, Djureinovic D, Odeberg J, Habuka M, Tahmasebpoor S, Danielsson A, Edlund K, Asplund A, Sjöstedt E, Lundberg E, Szigyarto CA, Skogs M, Takanen JO, Berling H, Tegel H, Mulder J, Nilsson P, Schwenk JM, Lindskog C, Danielsson F, Mardinoglu A, Sivertsson A, von Feilitzen K, Forsberg M, Zwahlen M, Olsson I, Navani S, Huss M, Nielsen J, Ponten F and Uhlén M. Analysis of the human tissue-specific expression by genome-wide integration of transcriptomics and antibody-based proteomics. Mol Cell Proteomics 2014; 13: 397-406.
[14] Lv D, Chen Y, Tang L, Tian Y, Ren D, Jian N and Shen T. HECTD2/TNFAIP1 axis regulating the p38/JNK pathway to promote an inflammatory response in renal cell carcinoma cells. In Vivo 2024; 38: 1094-1103.
[15] Li L, Zhang W, Liu Y, Liu X, Cai L, Kang J, Zhang Y, Chen W, Dong C, Zhang Y, Wang M, Wei W and Jia L. The CRL3(BTBD9) E3 ubiquitin ligase complex targets TNFAIP1 for degradation to suppress cancer cell migration. Signal Transduct Target Ther 2020; 5: 42.
[16] Liu Y, Zhang W, Wang S, Cai L, Jiang Y, Pan Y, Liang Y, Xian J, Jia L, Li L, Zhao H and Zhang Y. Cullin3-TNFAIP1 E3 Ligase controls inflammatory response in hepatocellular carcinoma cells via ubiquitination of RhoB. Front Cell Dev Biol 2021; 9: 617134.
[17] Xiao Y, Huang S, Qiu F, Ding X, Sun Y, Wei C, Hu X, Wei K, Long S, Xie L, Xun Y, Chen W, Zhang Z, Liu N and Xiang S. Tumor necrosis factor α-induced protein 1 as a novel tumor suppressor through selective downregulation of CSNK2B blocks nuclear factor-κB activation in hepatocellular carcinoma. EBioMedicine 2020; 51: 102603.
[18] Han JH, Lee YS, Kim HJ, Lee SY and Myung SC. Association between cytochrome CYP17A1, CYP3A4, and CYP3A43 polymorphisms and prostate cancer risk and aggressiveness in a Korean study population. Asian J Androl 2015; 17: 285-291.
[19] Sevrioukova IF and Poulos TL. Understanding the mechanism of cytochrome P450 3A4: recent advances and remaining problems. Dalton Trans 2013; 42: 3116-3126.
[20] Zhang Y, Wang Z, Wang Y, Jin W, Zhang Z, Jin L, Qian J and Zheng L. CYP3A4 and CYP3A5: the crucial roles in clinical drug metabolism and the significant implications of genetic polymorphisms. PeerJ 2024; 12: e18636.
[21] Yi-Wen Z, Mei-Hua B, Xiao-Ya L, Yu C, Jing Y and Hong-Hao Z. Effects of oridonin on hepatic cytochrome P450 expression and activities in PXR-humanized mice. Biol Pharm Bull 2018; 41: 707-712.
[22] Sabarathinam S and Ganamurali N. Hyperforin as a non-steroidal modulator of the PXR-CYP3A4 regulatory axis: mechanistic and computational insights into xenobiotic metabolism. J Steroid Biochem Mol Biol 2026; 256: 106886.
[23] Chen W, Zhang F, Xu H, Hou X, Tang D and Dai Y. Identification and characterization of genes related to the prognosis of hepatocellular carcinoma based on single-cell sequencing. Pathol Oncol Res 2022; 28: 1610199.
[24] Ma X, Zhou L and Zheng S. Transcriptome analysis revealed key prognostic genes and mi-

croRNAs in hepatocellular carcinoma. PeerJ 2020; 8: e8930.
[25] Tabata Y. Geranylgeranoic acid and the MAOB-CYP3A4 axis: a metabolic shift underlying age-related liver cancer risk. Front Aging 2025; 6: 1680031.
[26] Augustin E, Pawłowska M, Polewska J, Potega A and Mazerska Z. Modulation of CYP3A4 activity and induction of apoptosis, necrosis and senescence by the anti-tumour imidazoacridinone C-1311 in human hepatoma cells. Cell Biol Int 2013; 37: 109-120.
[27] Nouri K, Piryaei A, Seydi H, Zarkesh I, Ghoytasi I, Shokouhian B, Najimi M and Vosough M. Fibrotic liver extracellular matrix induces cancerous phenotype in biomimetic micro-tissues of hepatocellular carcinoma model. Hepatobiliary Pancreat Dis Int 2025; 24: 92-103.
[28] Carlessi R, Köhn-Gaone J, Olynyk JK and Tirnitz-Parker JEE. Mouse models of hepatocellular carcinoma. In: Tirnitz-Parker JEE, editors. Hepatocellular Carcinoma. Brisbane (AU): Codon Publications Copyright: The Authors.; 2019.
[29] Sha J, Zhang R, Fan J, Gu Y, Pan Y, Han J, Xu X, Ren S and Gu J. The B-cell-specific ablation of B4GALT1 reduces cancer formation and reverses the changes in serum IgG glycans during the induction of mouse hepatocellular carcinoma. Cancers (Basel) 2022; 14: 1333.
[30] Uehara T, Ainslie GR, Kutanzi K, Pogribny IP, Muskhelishvili L, Izawa T, Yamate J, Kosyk O, Shymonyak S, Bradford BU, Boorman GA, Bataller R and Rusyn I. Molecular mechanisms of fibrosis-associated promotion of liver carcinogenesis. Toxicol Sci 2013; 132: 53-63.
[31] Mokhosoev IM, Astakhov DV, Terentiev AA and Moldogazieva NT. Human cytochrome P450 cancer-related metabolic activities and gene polymorphisms: a review. Cells 2024; 13: 1958.
[32] Wang J, Wang Y, Xu J, Song Q, Shangguan J, Xue M, Wang H, Gan J and Gao W. Global analysis of gene expression signature and diagnostic/prognostic biomarker identification of hepatocellular carcinoma. Sci Prog 2021; 104: 368504211029429.
[33] Zhang R, Huang M, Wang H, Wu S, Yao J, Ge Y, Lu Y and Hu Q. Identification of potential biomarkers from hepatocellular carcinoma with MT1 deletion. Pathol Oncol Res 2021; 27: 597527.
[34] Mao Y, He JX, Zhu M, Dong YQ and He JX. Correction to: circ0001320 inhibits lung cancer cell growth and invasion by regulating TNFAIP1 and TPM1 expression through sponging miR-558. Hum Cell 2021; 34: 1287.
[35] Liu CL, Lim YP and Hu ML. Fucoxanthin attenuates rifampin-induced cytochrome P450 3A4 (CYP3A4) and multiple drug resistance 1 (MDR1) gene expression through pregnane X receptor (PXR)-mediated pathways in human hepatoma HepG2 and colon adenocarcinoma LS174T cells. Mar Drugs 2012; 10: 242-257.
[36] Diab T, Alkafaas SS, Shalaby TI and Hessien M. Paclitaxel nanoparticles induce apoptosis and regulate TXR1, CYP3A4 and CYP2C8 in breast cancer and hepatoma cells. Anticancer Agents Med Chem 2020; 20: 1582-1591.
[37] Lu C, Fang S, Weng Q, Lv X, Meng M, Zhu J, Zheng L, Hu Y, Gao Y, Wu X, Mao J, Tang B, Zhao Z, Huang L and Ji J. Integrated analysis reveals critical glycolytic regulators in hepatocellular carcinoma. Cell Commun Signal 2020; 18: 97.
[38] Aoki T, Nishida N, Kurebayashi Y, Sakai K, Fujiwara N, Tsurusaki M, Hanaoka K, Morita M, Chishina H, Takita M, Hagiwara S, Ida H, Ueshima K, Minami Y, Takebe A, Murase T, Kamei K, Nakai T, Matsumoto I, Nishio K and Kudo M. Molecular classification of hepatocellular carcinoma based on zoned metabolic feature and oncogenic signaling pathway. Clin Mol Hepatol 2025; 31: 981-1002.
[39] Chen H, Shen ZY, Xu W, Fan TY, Li J, Lu YF, Cheng ML and Liu J. Expression of P450 and nuclear receptors in normal and end-stage Chinese livers. World J Gastroenterol 2014; 20: 8681-8690.

Table S1. Primer sequences

Gene	Primer (5'-3')
H-TNFAIP1-F	GGGTTGGGCAACAAGTATGTC
H-TNFAIP1-R	GGTGTCATCTCGGAGGTAATTCA
H-CYP3A4-F	CACGAGCAGTGTTCTCTCCTT
H-CYP3A4-R	CACAGTATCATAGGTGGGTGGT
H-PXR-F	TGTTCAAAGGCATCATCAGC
H-PXR-R	CACTCCCAGGTTCCAGTCTC
H-GAPDH-F	CTGGGCTACACTGAGCACC
H-GAPDH-R	AAGTGGTCGTTGAGGGCAATG
M-Tnfaip1-F	GCCCAAGATCAGTGGCTTCAA
M-Tnfaip1-R	GTGCTTTCCACATCGGTCTATG
M-Cyp3a11-F	AGTGTGGTGCCTTACAGAGC
M-Cyp3a11-R	GGAGAGGCGTTTGACCATCA
M-Pxr-F	TCCCTCTTCTCCCCAGATCG
M-Pxr-R	GTGAGGGCAAACCTCTCCTG
M-Afp-F	CCAGGAAGTCTGTTTCACAGAAG
M-Afp-R	CAAAAGGCTCACACCAAAGAG
M-Fgf21-F	GACGACCAAGACACTGAAGC
M-Fgf21-R	GGATTTGAATGACCCCTGGC
M-Ccnd1-F	TAGGCCCTCAGCCTCACTC
M-Ccnd1-R	CCACCCCTGGGATAAAGCA
M-C3-F	CCAGCTCCCCATTAGCTCTG
M-C3-R	GCACTTGCCTCTTTAGGAAGTC
M-C5-F	GAACAAACCTACGTCATTTCAGC
M-C5-R	GTCAACAGTGCCGCGTTTT
M-IL-1β-F	TGGACCTTCCAGGATGAGGACA
M-IL-1β-R	GTTCATCTCGGAGCCTGTAGTG
M-IL-6-F	CCAAGAGGTGAGTGCTTCCC
M-IL-6-R	CTGTTGTTCAGACTCTCTCCCT
M-Gapdh-F	AGGTCGGTGTGAACGGATTTG
M-Gapdh-R	TGTAGACCATGTAGTTGAGGTCA

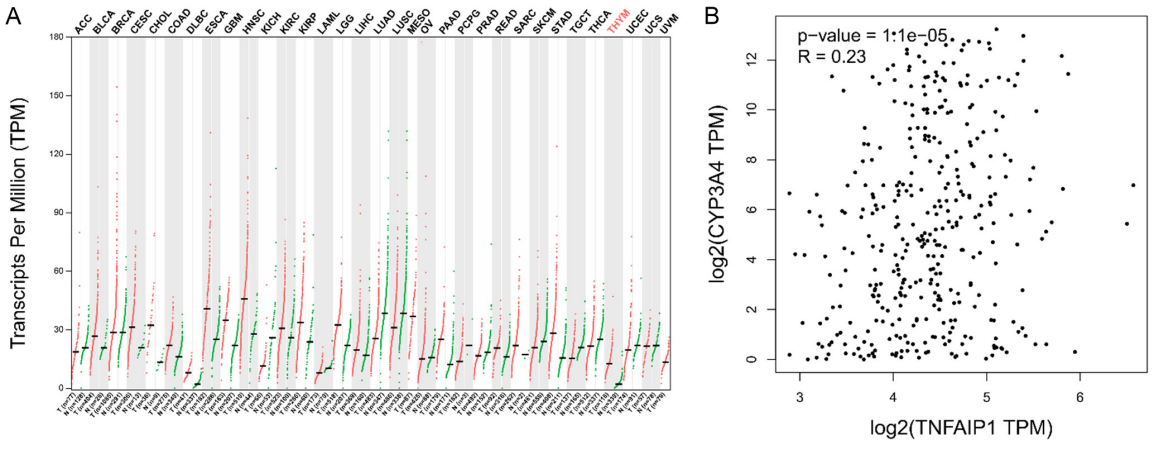

Figure S1. Analysis of TNFAIP1 expression and its correlation with CYP3A4 in pan-cancer and HCC. A. Differential expression of TNFAIP1 gene in tumor versus non-tumor tissues from patients with various cancers; B. Correlation between TNFAIP1 and CYP3A4 expression in HCC patients from the TCGA-LIHC cohort.

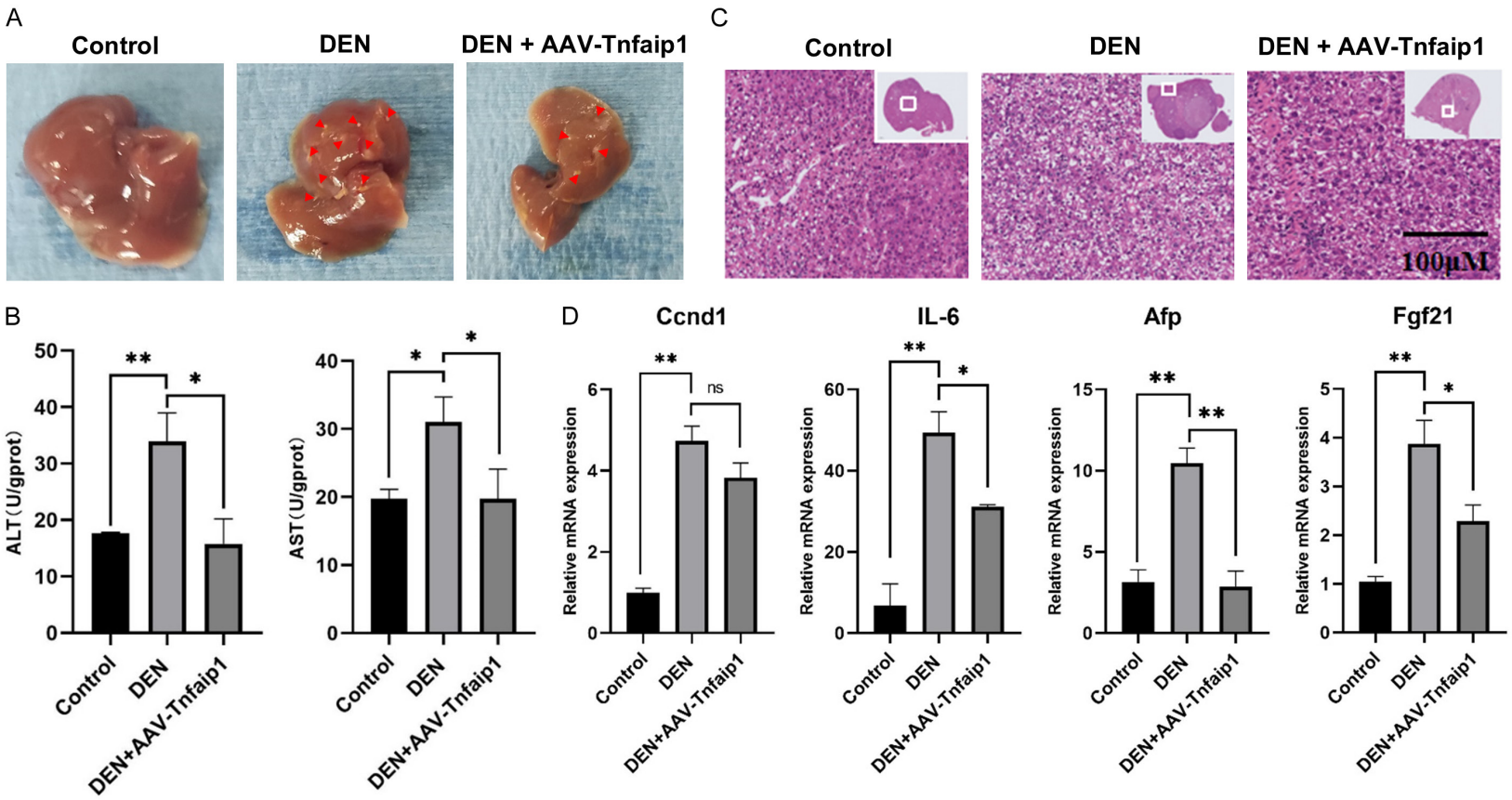

Figure S2. Tnfaip1 overexpression alleviates DEN/CCl4-induced mouse HCC phenotypes. A. Histomorphology of mouse liver (nodules indicated by red arrows); B. Serum ALT and AST levels in mice; C. HE staining results of mouse liver sections (scale bar = 100 μm; Magnification: ×200); D. mRNA levels of Afp, Ccnd1, Fgf21, and IL-6 in mouse liver tissue. $^{*}P < 0.05$, $^{**}P < 0.01$.

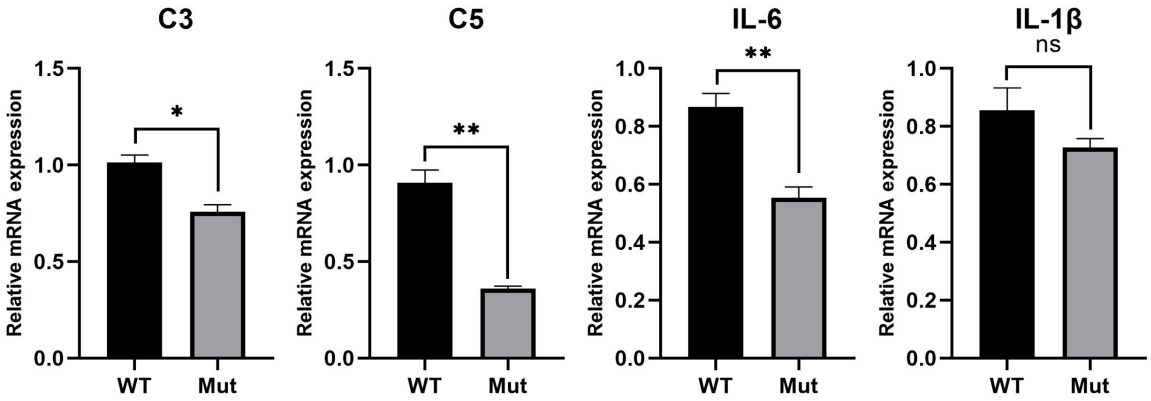

Figure S3. Tnfaip1 knockout affects basal immune and inflammatory states in mouse liver. mRNA levels of C3, C5, IL-1β, and IL-6 in liver tissue from WT and Mut mice. $^{*}P < 0.05$, $^{**}P < 0.01$.